

Divergence of hydraulic traits among tropical forest trees across topographic and vertical environment gradients in Borneo

Paulo Roberto de Lima Bittencourt¹ , David C. Bartholomew^{1,2}, Lindsay F. Banin³ ,
Mohamed Aminur Faiz Bin Suis⁴, Reuben Nilus⁴, David F. R. P. Burslem⁵ and Lucy Rowland¹ 

¹College of Life and Environmental Sciences, University of Exeter, Exeter, EX4 4QE, UK; ²Department of Ecology and Environmental Science, Umeå University, 90736 Umeå, Sweden;

³UK Centre for Ecology & Hydrology, Penicuik, Midlothian, EH26 0QB, UK; ⁴Sabah Forestry Department, Forest Research Centre, PO Box 1407, Sandakan, 90715, Sabah, Malaysia;

⁵School of Biological Sciences, University of Aberdeen, Aberdeen, AB24 3UU, UK

Summary

Author for correspondence:
Paulo Roberto de Lima Bittencourt
Email: paulo09d@gmail.com

Received: 24 February 2022
Accepted: 23 May 2022

New Phytologist (2022)
doi: 10.1111/nph.18280

Key words: Dipterocarpaceae, hydraulic traits, large trees, niche specialization, Southeast Asia, tree height, tropical forest, water transport.

- Fine-scale topographic–edaphic gradients are common in tropical forests and drive species spatial turnover and marked changes in forest structure and function. We evaluate how hydraulic traits of tropical tree species relate to vertical and horizontal spatial niche specialization along such a gradient.
- Along a topographic–edaphic gradient with uniform climate in Borneo, we measured six key hydraulic traits in 156 individuals of differing heights in 13 species of Dipterocarpaceae. We investigated how hydraulic traits relate to habitat, tree height and their interaction on this gradient.
- Embolism resistance increased in trees on sandy soils but did not vary with tree height. By contrast, water transport capacity increased on sandier soils and with increasing tree height. Habitat and height only interact for hydraulic efficiency, with slope for height changing from positive to negative from the clay-rich to the sandier soil. Habitat type influenced trait–trait relationships for all traits except wood density.
- Our data reveal that variation in the hydraulic traits of dipterocarps is driven by a combination of topographic–edaphic conditions, tree height and taxonomic identity. Our work indicates that hydraulic traits play a significant role in shaping forest structure across topographic–edaphic and vertical gradients and may contribute to niche specialization among dipterocarp species.

Introduction

Tropical forests are highly diverse ecosystems hosting an estimated 40 000–50 000 tree species across the biome (Slik *et al.*, 2015). Fine-scale habitat variability is an important driver of tropical forest diversity, structure and function. Within the same microclimatic envelope, differences in edaphic conditions, which are often associated with topographic changes, can lead to almost complete species turnover (Baldeck *et al.*, 2013; Schietti *et al.*, 2014; Guitet *et al.*, 2015). The species turnover is often associated with a sharp change in forest structure and functioning (Lee *et al.*, 2002; Cosme *et al.*, 2017; Jucker *et al.*, 2018). Forest structural changes across fine-grained topographic–edaphic gradients often follow the same patterns as those found at large spatial scales in the tropics, for example shorter trees in dry sites and on well-drained and nutrient-poor soils (Feldpausch *et al.*, 2011). This change in forest structure can lead to large differences in biomass across these gradients (Ferry *et al.*, 2010; Jucker *et al.*, 2018). Topographic–edaphic variability can also drive fine-scale differences in growth and mortality patterns, drought sensitivity and species reproductive phenology across the landscape (Itoh

et al., 2003, 2012; Ferry *et al.*, 2010; Esteban *et al.*, 2021). Due to their fine spatial scale, these gradients are often neglected in large-scale studies, despite their important influence on tropical forest function. For example, *c.* 40% of forests in Amazonia are situated in valleys and function differently to those in upland plateau environments at the same general location; however, they are treated as a single forest in most vegetation models (Oliveira *et al.*, 2019; Esteban *et al.*, 2021). As such, understanding the principles governing the evolution, community assembly and function of forests on local environmental gradients is fundamental to understanding and predicting ecosystem processes.

Plant hydraulic traits have significant potential to explain plant species distribution and functioning at both global and local scales (Blackman *et al.*, 2011; Trueba *et al.*, 2017; Oliveira *et al.*, 2019; Laughlin *et al.*, 2020). They directly control the efficiency with which plants can transport water and resist soil and/or atmospheric drought, as well as influencing nutrient uptake and carbon assimilation rates (Sperry & Love, 2015; Christoffersen *et al.*, 2016). Critically, hydraulic traits constrain the relationship between abiotic (climate and soil) conditions and stomatal conductance (Sperry & Love, 2015; Eller *et al.*, 2020). This in turn

sets limitations on key aspects of plant architecture such as maximum height, allometry and branching patterns (West *et al.*, 1999; Sperry *et al.*, 2008; Christoffersen *et al.*, 2016) and canopy physiology (Brodribb *et al.*, 2017). Hydraulic traits also play a key role in plant evolution and niche specialization (Larter *et al.*, 2017; Sanchez-Martinez *et al.*, 2020). In the Central Amazon, rapid species turnover along a fine-scale topographic gradient (< 1 km) is explained by habitat filtering based on hydraulic traits; trees are highly specialised to the edaphic conditions, with contrasting communities found in drier hills and wetter valleys (Cosme *et al.*, 2017; Oliveira *et al.*, 2019). Traits related to how efficiently plants transport water and resist drought stress are highlighted as key controls on Amazonian species' habitat associations (Esquivel-Muelbert *et al.*, 2017; Trueba *et al.*, 2017; Oliveira *et al.*, 2019); however, whether this is general across the tropics and in the less seasonal Southeast Asian tropical forests is still unknown.

The efficiency with which a plant can transport water through its xylem is often measured as the hydraulic conductivity of the xylem, which is proportional to conduit diameter and length (Sperry *et al.*, 2008). Trees located on persistently dry soils are likely to have conservative resource acquisition strategies and are unlikely to need a high degree of hydraulic efficiency for sustaining photosynthesis (Oliveira *et al.*, 2021). These trees are usually shorter with narrower and shorter conduits (Santiago *et al.*, 2004; Zhang & Cao, 2009; Christoffersen *et al.*, 2016; Olson *et al.*, 2021). Drier environments are also likely to favour xylem tissue with a greater capacity to resist embolism and therefore hydraulic failure (Choat *et al.*, 2007; Blackman *et al.*, 2014; Trueba *et al.*, 2017; Oliveira *et al.*, 2019). Xylem embolism resistance is often measured as the xylem water potential that causes 50% or 88% of water transport capacity loss (P50 and P88, respectively; Cruiziat *et al.*, 2002; Pérez-Harguindeguy *et al.*, 2013). Traits that integrate metrics of allocation to water-demanding and carbon-acquiring tissues (leaf area) relative to allocation to water supply capacity (xylem area) are also important integrators of these two key traits (Mencuccini *et al.*, 2019). Two traits frequently used to quantify this are the leaf : sapwood area ratio (LS), the leaf area allocation per unit transversal area of water transporting tissue, and the leaf specific hydraulic conductivity, which is the xylem hydraulic conductivity per leaf area it supplies. While they are not perfect proxies for hydraulic capacity, as they do not account for branch volume, these traits provide key information on plant hydraulic strategy (Mencuccini *et al.*, 2019). All of these hydraulic traits are likely to be strongly affected by soil texture, which is a major determinant of both the amount of soil water available to plants and the hydraulic conductivity connecting water to the roots (Hacke *et al.*, 2000; Li *et al.*, 2005; Pollacco *et al.*, 2020). Sandy soils are likely to be more hydraulically challenging than clay-rich soils (Hacke *et al.*, 2000, p. 200; Li *et al.*, 2005; Hultine *et al.*, 2006; Poepflau & Kätterer, 2017); however, this may not always be purely related to soil physical properties. The loss of root contact with the soil particles as soils dry can also be a key bottleneck for water uptake from the sandier soils (Herkeleth *et al.*, 1977a,b; Li *et al.*, 2005; Fisher *et al.*, 2007).

Bornean forests have the highest aboveground biomass density of any tropical forest (Avitabile *et al.*, 2016), partly because the trees typically attain greater maximum heights and are taller for a given diameter (Banin *et al.*, 2012). These features are linked to the prevalence of the Dipterocarpaceae family, which is both highly diverse and contains the tallest known tropical trees on Earth (Brearley *et al.*, 2016; Jucker *et al.*, 2018; Shenkin *et al.*, 2019), attaining maximum heights in excess of 100 m (Shenkin *et al.*, 2019). This requires a robust hydraulic system that is capable of overcoming the increase in hydraulic resistance from the soil to the leaves (Sperry *et al.*, 2008; Savage *et al.*, 2010; McDowell & Allen, 2015). For each 10 m in height, gravity increases the tension in the xylem water column by *c.* 0.1 MPa which, added to the increased resistance from a longer hydraulic pathway, puts taller trees under greater risk of hydraulic failure (Cruiziat *et al.*, 2002). Consequently, the hydraulic system of tall trees often differs from that of shorter trees, with taller trees having to develop a more efficient and safer system (Fajardo *et al.*, 2019; Liu *et al.*, 2019; Olson *et al.*, 2021). However, evidence suggests some tall tropical trees either have the same hydraulic traits as shorter trees, or have a less resistant hydraulic system, because of a height related constraint on their capacity to maintain their hydraulic resistance (Rowland *et al.*, 2015; Bittencourt *et al.*, 2020). If tall trees fail to adjust their hydraulic traits to keep up with the increasing stresses imposed by height, they will rapidly become increasingly susceptible to drought-induced mortality as they grow (Nepstad *et al.*, 2007; Phillips *et al.*, 2010; Bennett *et al.*, 2015; Ryan, 2015). This could explain why, in Borneo, the tallest dipterocarp species do not occur on soils with a very high sand content, where water is likely more limiting (Herkeleth *et al.*, 1977a; Li *et al.*, 2005). If true, this group of species may also be most at risk from the drier conditions expected with climate change (Dai, 2013).

Dipterocarps account for a low proportion of Bornean tree diversity (Slik *et al.*, 2003) but represent a high proportion of aboveground carbon stocks – up to 60% of forest basal area (Ghazoul, 2016). However, dipterocarps are not found uniformly across the landscape, as the structure of these forests is highly variable across fine spatial scales. The dipterocarp forests in Borneo display marked variation in species composition and function across topographic–edaphic gradients, which are associated with species turnover and changes in forest structure (Paoli *et al.*, 2006; Sukri *et al.*, 2012; Brearley *et al.*, 2016; Jucker *et al.*, 2018). In the Sepilok Forest Reserve in Sabah, northeast Borneo, changes in edaphic properties with topography at fine spatial scales (< 1 km), drive transitions from tall forests, growing on nutrient rich and clayey soils, where dipterocarps exceed 80 m in height, to low canopy height forests, located on very sandy soils, where trees reach no more than 40 m in height (Dent *et al.*, 2006; Jucker *et al.*, 2018). These transitions also lead to an almost complete turnover in dipterocarp species (Nilus, 2004; Brearley *et al.*, 2016). Consequently, the species turnover and high beta diversity of these forests can largely be attributed to changing soil conditions. To date, however, there have been limited studies that evaluate how plant traits related to key functional processes, such as water transport and carbon assimilation,

vary across such gradients, particularly in Bornean forests. This limits our capacity to understand the physiological and evolutionary drivers of niche specialization. The handful of functional trait studies from topographic–edaphic gradients in Borneo which measure water-use efficiency, leaf respiration and carbon and nutrient allocation strategies do suggest that there are strong selective pressures on plant function across these gradients, but these have focussed on juvenile size classes of trees and relatively few species (Baltzer *et al.*, 2005; Dent & Burslem, 2009, 2016; Russo *et al.*, 2010; Katabuchi *et al.*, 2012). Tyree *et al.* (1998) present the only study, to our knowledge, of hydraulic traits in Bornean forests. They found no significant change in xylem embolism resistance from more clay rich alluvial to sandier heath forests in Brunei, which supports theoretical expectations that in sites where soil–rhizosphere connections are the hydraulic bottleneck, there is no advantage for trees to have high embolism resistance, unless root : leaf area is simultaneously increased relative to non-soil–rhizosphere limited sites (Sperry *et al.*, 1998). However, Tyree *et al.* (1998) focused only on juvenile trees of both dipterocarp and nondipterocarp species, studying only one individual of 14 distinct species at each site, making it challenging to draw more general conclusions.

In this study, we address whether variation in dipterocarp hydraulic traits is determined by topographic–edaphic environments, tree height and their interaction using the edaphic-topographic gradient in the Sepilok Forest reserve as our study system. We ask whether hydraulic traits controlling embolism resistance (hydraulic safety) and water transport efficiency and capacity can explain the high frequency of niche specialization and spatial turnover of Bornean dipterocarps, as well as the large size differences observed amongst dipterocarp species across habitat types on these gradients. We measured hydraulic traits in 156

individuals of varying heights, starting from 5 m as a minimum threshold, in 13 dipterocarp species across a topographic–edaphic gradient where soils change from clay and nutrient-rich (alluvial forest) to sandy and nutrient-poor (sandstone and kerangas forests, sequentially; Fig. 1) across a distance of *c.* 5 km. We tested the following hypotheses:

- (1) Forests with higher soil water availability (alluvial forests) have selected for dipterocarp species with higher water transport efficiency and lower hydraulic safety (i.e. higher hydraulic conductance, higher LS and lower embolism resistance) than forests on well-drained sandier soils (sandstone and kerangas forests).
- (2) Dipterocarp species adjust their hydraulic traits to become safer and more efficient with increasing size, and this adjustment is different across forest types with different soil conditions. We predict that hydraulic efficiency and embolism resistance increase and LSs decrease with tree height, with these traits scaling more strongly in the alluvial forest, where taller stature requires greater hydraulic adjustments.
- (3) Topographic–edaphic gradients not only select for specific hydraulic traits, but also change the magnitude of hydraulic trait–trait coordination or trade-offs. We predict the slopes of the relationships between hydraulic traits are steeper in the kerangas forest, as water shortage selects for more extreme values of hydraulic traits in this environment.

Materials and Methods

Site and sampling

This study was conducted in the Kabili-Sepilok Forest Reserve, northeast Borneo (lat. 5°52′ 34″N, long. 117°56′58″E). The landscape is composed of mixed dipterocarp and kerangas forest,

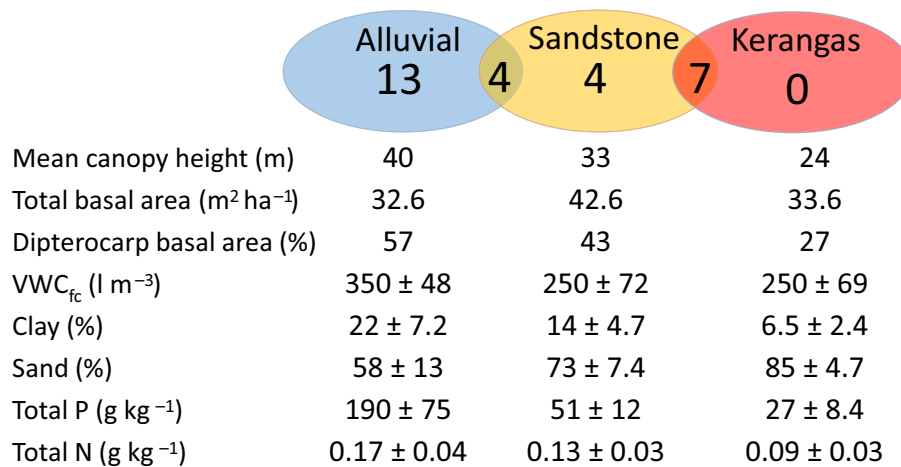


Fig. 1 Biotic, physical and chemical descriptions of the three studied forest types (from Nilus, 2004, Jucker *et al.*, 2018; Bartholomew *et al.*, 2022). The numbers in the Venn diagram indicate the total dipterocarp species richness for species with at least 1 individual ha⁻¹ occurring in each forest type. Numbers in the intersections between ellipses indicate the number of species occurring in both environments with at least 1 individual ha⁻¹. No species co-occur in the alluvial and kerangas forests with at least 1 individual ha⁻¹. The table shows forest structure indices (mean canopy height, total basal area and percentage dipterocarp basal area in relation to the total for stems ≥ 5 cm diameter at breast height), and soil properties. Forest structure is from a 36 ha forest inventory (12 ha per forest type) with all trees ≥ 5 cm diameter measured; the total number of dipterocarp species in the census is 67, of which 28 have > 1 individual ha⁻¹. The description of soil physical and chemical attributes for the different studied forests is presented in terms of mean values ± SD for 75 soil collection points, at 5 cm depth, per forest type. N, nitrogen; P, phosphorus; VWC_{fc}, soil volumetric water content at field capacity (VWC measured *c.* 12 h after a strong rainfall event, ensuring enough time for drainage so soil would be saturated and not super saturated).

with a mean monthly temperature of $26.5 \pm 0.6^\circ\text{C}$ (mean \pm SD) and a mean annual precipitation of 2640 ± 675 mm (Copernicus Climate Change Service, 2019). Dry spells occur infrequently, although monthly precipitation rarely falls below 100 mm (Supporting Information Fig. S1). Within our site, there are nine permanent 4 ha plots, comprising three plots located in each of the three forest types defined here as alluvial, sandstone and kerangas (Fig. 1; see (Nilus, 2004, for details). The alluvial forest covers the lowland flat valleys and embedded low mudstone hills and is characterised by nutrient rich and clayey soils. The sandstone forest is located on steep hillsides and ridges and is intermediate in terms of soil nutrient and water availability between the alluvial and kerangas forest, with a high diversity of dipterocarp species but lower total dipterocarp canopy height (Jucker *et al.*, 2018). The kerangas forest occurs on podzols with associated cuesta dip slopes; soils are nutrient-poor with a high sand content, and plant communities have a low diversity (see Fox, 1975; Baltzer *et al.*, 2005; Dent *et al.*, 2006 for details; Fig. 1).

We collected samples from the canopies of 6–16 individuals of different heights from between 4 and 7 dipterocarp species in each forest type (total of 13 species and 156 individuals across all habitats) from July to September 2018. Sunlit branches 1.5–2 m long were cut from the canopy by experienced climbers and transported in moist plastic bags to a laboratory 30–60 min walk from each plot, where they were processed within 1–4 h of being cut to avoid artefacts. Our species selection comprised the most abundant dipterocarp species in each forest type: *Cotylelobium melanoxylon* (Hook.f.) Pierre, *Dipterocarpus acutangulus* Vesque, *Dipterocarpus caudiferus* Merr., *Dipterocarpus grandiflorus* (Blanco) Blanco, *Dipterocarpus kunstleri* King, *Hopea beccariana* Burck, *Parashorea tomentella* (Symington) Meijer, *Shorea johorensis* Foxw., *Shorea macroptera* Dyer, *Shorea multiflora* (Burck) Symington, *Shorea smithiana* Symington, *Shorea xanthophylla* Symington and *Vatica micrantha* Slooten. A summary of the sampling design is presented in Table 1 and species' abundances per forest type are shown in Table S1. *Shorea macroptera*, *S. smithiana*, *S. multiflora* and *H. beccariana* were abundant in more than one habitat type (dominance rank < 30; Tables 1, S1) and we sampled these in both environments. For each tree, we measured diameter at breast height using a metric tape and tree height using the sine method (Larjavaara & Muller-Landau, 2013) with a laser distance meter (Forestry Pro II; Nikon, Tokyo, Japan). For wood density and LS, we used an extended dataset with *c.* 10–26 individuals of varying height collected for each of the 13 species in each forest type.

Embolism resistance

We measured embolism resistance to xylem tension using the pneumatic method to estimate the amount of xylem embolism and the bench dehydration method to induce embolism (Pereira *et al.*, 2016). The pneumatic method measures embolism by extracting air from embolized vessels and quantifying the increase in extracted air during sample desiccation (Zhang *et al.*, 2018; Yang *et al.*, 2021). While the pneumatic method has not been

tested across as many ecosystems as other methods, values of embolism resistance obtained using this method are strongly correlated with those made using other methods and are unlikely to be systematically biased (Pereira *et al.*, 2016; Zhang *et al.*, 2018; Sergent *et al.*, 2020; Guan *et al.*, 2021; Paligi *et al.*, 2021).

We used terminal branches 40–70 cm long for the pneumatic method measurements. We recut collected samples under water and left them to rehydrate overnight before starting measurements. The following day, samples were connected to an automated pneumatic apparatus (M-Pneumatron) which applies a vacuum and monitors pressure in the sample for 150 s (Pereira *et al.*, 2019). We calculated the volume of gas discharged from the sample for each measurement using the ideal gas law. We calculated the percentage gas discharge (PGD), an estimate of xylem embolism and a proxy of xylem percentage loss of hydraulic conductance, by standardizing each gas discharge measurement of a sample by its minimum and maximum value. We used three M-Pneumatrons, each measuring the gas discharge of 10 samples for 2–4 d, depending on sample desiccation time, with each sample being measured once every 30 min. We stopped measuring a sample when its water potential was < -9 MPa (Bittencourt *et al.*, 2018).

We estimated xylem water potential by measuring the water potential of leaves equilibrated with the xylem by stopping their transpiration. To allow for this equilibration period to take place, the branches were bagged in thick plastic sacks for 1 h, before leaf water potential was measured with a pressure chamber (Model 1515D; PMS, Albany, NY, USA; Scholander *et al.*, 1964). We used P50 and P88, the water potential values leading to 50% and 88% hydraulic failure in the xylem, as indices of xylem embolism resistance; they were estimated by fitting PGD to xylem water potential using a sigmoidal equation and extracting the estimated P50 and P88 data points (Pammenter & Vander, 1998; Fig. S2).

Maximum hydraulic conductance

We measured maximum hydraulic conductivity (K_s) on small (3–5 cm long) distal branch samples using the hydraulic setup described by Sperry *et al.* (1988). This method consists of measuring the sample conductance by applying a known water pressure and quantifying the water flow rate it causes through the sample. Sample conductance is then standardized to sample specific conductivity (K_s) by multiplying by its length and dividing by its transverse area. An ideal measurement of K_s requires all vessels in the sample to be closed, so the conductance is representative of both vessel lumen and pit membrane conductivity. For tropical trees, mean vessel length is often longer than 10 cm and maximum vessel length is often longer than 1 m (Jacobsen *et al.*, 2012), which makes measurement of samples with all vessels closed unfeasible. Thus, we decided to use the shortest samples possible (3–5 cm), to ensure that most of the vessels were open and to reduce bias associated to this (Melcher *et al.*, 2012). When using very short samples, while species with different vessel lengths will still have some difference in the percentage of closed vessels, most of the vessels will still be open and this difference is unlikely to cause biases. Using the K_s measured in this way (vessel

Table 1 Summary of traits measured for each dipterocarp species in each environment.

Forest	Species	P50	P88	K_s	K_{sl}	LS	WD	DBH	Height	H range	n	$n K_s$	n WD
Alluvial	<i>Dipterocarpus caudiferus</i>	-2.2 ± 0.2	-2.6 ± 0.41	0.6 ± 0.33	0.0017 ± 0.0012	0.00046 ± 0.00012	0.6 ± 0.11	32 ± 36	20 ± 15	7.8–58	9	7	16
	<i>Dipterocarpus kunstleri</i>	-2.1 ± 0.32	-2.9 ± 0.54	0.55 ± 0.28	0.0014 ± 0.0013	0.00052 ± 0.00021	0.57 ± 0.053	25 ± 17	19 ± 8.8	7.9–42	12	8	17
	<i>Parashorea tomentella</i>	-2.6 ± 0.43	-3.4 ± 0.81	0.62 ± 0.4	0.0016 ± 0.0014	0.00047 ± 0.00021	0.45 ± 0.11	33 ± 25	31 ± 20	7.2–66	16	15	27
	<i>Shorea johorensis</i>	-2 ± 0.22	-2.6 ± 0.24	0.91 ± 0.24	0.0015 ± 0.0063	0.00061 ± 0.00016	0.42 ± 0.062	97 ± 27	54 ± 8	38–62	4	4	6
	<i>Shorea macroptera</i>	-2.3 ± 0.21	-3 ± 0.28	0.4 ± 0.14	0.0057 ± 0.0028	0.00048 ± 0.0002	0.46 ± 0.076	56 ± 27	20 ± 14	7.5–43	6	4	9
	<i>Shorea smithiana</i>	-2.2 ± 0.18	-2.7 ± 0.51	0.67 ± 0.24	0.0024 ± 0.0015	0.00052 ± 0.00024	0.45 ± 0.099	60 ± 30	43 ± 18	15–63	4	4	13
Sandstone	<i>Shorea xanthophylla</i>	-3 ± 0.42	-3.9 ± 0.69	0.26 ± 0.11	0.004 ± 0.0022	0.00062 ± 0.00022	0.52 ± 0.074	41 ± 27	21 ± 8.1	9.5–30	11	11	18
	<i>Dipterocarpus acutangulus</i>	-2.8 ± 0.33	-3.7 ± 0.65	0.51 ± 0.25	0.0011 ± 0.0083	0.00056 ± 0.00025	0.7 ± 0.064	40 ± 33	25 ± 14	6.7–44	8	13	17
	<i>Dipterocarpus grandiflorus</i>	-2.8 ± 0.66	-4.2 ± 0.86	0.34 ± 0.21	0.0011 ± 0.0010	0.00049 ± 0.00027	0.53 ± 0.084	31 ± 30	22 ± 12	7.3–41	14	15	24
	<i>Hopea beccariana</i>	-3.2 ± 0.12	-4.2 ± 0.5	0.55 ± 0.26	0.0095 ± 0.0046	0.00051 ± 0.00015	0.61 ± 0.051	31 ± 23	22 ± 13	5.1–40	4	2	14
	<i>Shorea macroptera</i>	-2.5 ± 0.63	-3.6 ± 0.88	0.41 ± 0.11	0.0066 ± 0.0033	0.00043 ± 0.00016	0.48 ± 0.058	24 ± 19	19 ± 11	4.4–45	10	4	19
	<i>Shorea multiflora</i>	-3.3 ± 0.44	-4.4 ± 0.74	0.32 ± 0.17	0.0062 ± 0.0077	0.00064 ± 0.00033	0.62 ± 0.079	38 ± 32	21 ± 12	6.5–49	10	11	16
Kerangas	<i>S. smithiana</i>	-2.4 ± 0.62	-3.4 ± 0.45	0.38 ± 0.15	0.0071 ± 0.0021	0.00051 ± 0.000078	0.4 ± 0.041	31 ± 24	24 ± 14	9.1–53	10	6	21
	<i>Cotylelobium melanoxylon</i>	-3.3 ± 0.3	-4.4 ± 0.84	0.69 ± 0.31	0.0026 ± 0.0020	0.00039 ± 0.00021	0.69 ± 0.058	32 ± 18	23 ± 10	7.2–42	14	22	34
	<i>H. beccariana</i>	-2.4 ± 0.26	-3.5 ± 0.64	0.74 ± 0.15	0.0033 ± 0.0015	0.00031 ± 0.00014	0.62 ± 0.094	22 ± 12	20 ± 7.4	10–30	4	4	10
	<i>S. multiflora</i>	-3 ± 0.64	-4.3 ± 1.1	0.39 ± 0.25	0.0011 ± 0.0010	0.0005 ± 0.00023	0.66 ± 0.042	28 ± 21	19 ± 7	5.2–26	13	20	24
	<i>Vatica micrantha</i>	-3.6 ± 0.23	-5.4 ± 0.22	0.33 ± 0.11	0.0010 ± 0.0057	0.029 ± 0.011	0.71 ± 0.048	24 ± 9.4	19 ± 5.4	8.6–29	3	6	14

Data presented are mean ± SD, except for 'H range', which reports the minimum and maximum values. 'n embolism', 'n K_s ' and 'n WD' are sample sizes for embolism resistance (P50 and P88); hydraulic conductivity and leaf : sapwood area (K_s , K_{sl} and LS); and wood density (WD), respectively. DBH, diameter at breast height (cm); H range, minimum and maximum tree height (m); height, tree height (m); K_s , maximum hydraulic specific conductivity ($\text{kg m}^{-2} \text{s}^{-1} \text{MPa}^{-1}$); K_{sl} , maximum hydraulic leaf-specific conductivity ($\text{kg m}^{-2} \text{s}^{-1} \text{MPa}^{-1}$); LS, leaf : sapwood area ratio ($\text{m}^2 \text{m}^{-2}$); P50, water potential causing a 50% reduction in hydraulic conductivity (MPa); P88, water potential causing an 88% reduction in hydraulic conductivity (MPa); WD, wood density (g cm^{-3}).

lumen K_s) should approximate potential maximum conductivity estimated from vessel diameter and number and provides an internally consistent dataset allowing us to identify patterns in the data, with the caveat that the values should not be compared with K_s measured in samples with closed vessels provided in other studies.

We flushed samples at *c.* 150 kPa for 30 s before conductance measurements to remove any emboli. Immediately after flushing, we measured sample conductance with a pressure of *c.* 150 kPa for another 30 s. Repeated flushing of a subset of samples for 30 s and measuring their conductance again did not lead to a further increase in conductance, indicating the 30 s flush was sufficient for the removal of all emboli. We used a custom thermal water flow meter in series with the sample to measure water flow (Miller & Small, 1982; Ashauer *et al.*, 1999; Methods S1).

Wood density and leaf : sapwood area

We measured wood density in 1–2 cm diameter samples by dividing their dry mass by their fresh volume. We removed the bark, rehydrated the samples overnight and measured their fresh volume by water volume displacement. We then dried the samples at 60°C for 48 h and measured their dry weight using an analytical scale. We measured the LS on the same samples used for K_{smax} measurements. We removed all leaves distal to the measured sample and scanned them to determine area using IMAGEJ (Schneider *et al.*, 2012) and the R package LEAFAREA (Katabuchi, 2015).

Data analysis

We tested whether the more nutrient-rich forest types (i.e. higher clay, soil water content and nutrient content) selected for species with more efficient and less safe hydraulic systems (hypothesis 1), and whether tree height affected hydraulic traits and whether tree height effects were modulated by forest type (hypothesis 2) using a linear mixed-effect model with species as a random variable affecting the intercept and/or the slope of the forest type and tree height fixed effects. We first selected the most parsimonious form of the random effect using the Akaike Information Criterion (AIC), with all fixed effects included. We tested for the significance of the random effect by comparing the full model with a model without random effects and assessed the significance of the difference between the models using a log-likelihood test (Zuur *et al.*, 2009). The contribution of each fixed effect in the model was then tested sequentially using a log-likelihood test against the full model with one fixed effect removed at a time (Zuur *et al.*, 2009; Thomas *et al.*, 2017). We tested whether hydraulic traits were interrelated and whether these relationships changed between forest types (hypothesis 3) using standard major axis regression, allowing forest type to affect the slope of the trait–trait relationship through an interaction term. If there was no difference in slopes, we then tested for differences in the intercept.

All analyses were performed in the R statistical environment (v.3.6; R Core Team, 2019). We used the package NLME for linear mixed effect models (Pinheiro *et al.*, 2014), the MUMIN package for the calculation of mixed model marginal and conditional pseudo- r^2 values (Barton, 2016) and the SMATR package for

standard major axis regression (Warton *et al.*, 2012). We log transformed K_{sleaf} and LS data to meet normality of residuals in mixed model analysis.

Results

Variation in hydraulic traits across forest types

Forest type, tree height and their interaction significantly affected hydraulic traits of the dipterocarps we sampled (Fig. 2; Table 2). Embolism resistance varied amongst forest types, such that P50 and P88 decreased progressively from the alluvial (for which mean \pm SEM for P50 and P88 were -2.50 ± 0.11 MPa and -3.10 ± 0.15 MPa, Fig. S2) to the sandstone (-2.82 ± 0.14 MPa and -4.384 ± 0.19 MPa) and to the kerangas forest (-2.91 ± 0.19 MPa and -4.27 ± 0.28 MPa, $P < 0.001$), following the gradient from periodically wet to consistently dry and freely draining sandy soils underlying these forest types. However, the difference between trees growing in sandstone and kerangas forest was not significant for either P50 or P88 ($P > 0.10$). Trees growing in the kerangas forest had higher hydraulic specific conductivity (K_s), higher leaf specific hydraulic conductivity (K_{sleaf}) and lower leaf : sapwood area (LS) than those growing in the alluvial and sandstone forests ($P < 0.001$ in all cases). Although median wood density was higher in the kerangas than in other forests (Fig. 2f), wood density was not significantly affected by forest type ($P = 0.12$). We note that pith size variability across wood density samples was negligible in our samples.

Tree height effects on hydraulic traits and their interaction with forest type

The heights of the trees we sampled varied from *c.* 5 to 66 m. The slopes of height (*y*) vs diameter (*x*) relationships from standardized major axis regression (SMA) were greater for trees in the alluvial forest than in either the sandstone ($P = 0.02$; Fig. S3) or kerangas ($P < 0.001$) forests, which scaled at a similar rate ($P = 0.23$). Using mixed effects models with tree height, forest type and their interaction as predictors (Table 2; Fig. 3), we found that K_s and K_{sleaf} were dependent on tree height (Table 2; Fig. 3) and that relationships between P50, wood density, LS and tree height varied amongst species (as indicated by the significant random slopes in these models). This suggests that even if we found no global relationship with height across all species, some species are likely to show stronger relationships than others (Fig. 4). There was no effect of height on P88. Maximum hydraulic specific conductivity (K_s) increased by 2.1% per m increase in tree height ($P < 0.001$), and K_{sleaf} increased by 1.3% per m increase in tree height ($P < 0.001$; % of K_s and K_{sleaf} in relation to the intercept; for K_{sleaf} , % is the value back-transformed from a \log_{10} scale). In addition to the direct tree height effect on K_s , with a slope of 0.28 for the intercept (i.e. alluvial forest), there was a significant interaction between forest type and tree height, with the sandstone forest having a shallower slope of 0.10 and the kerangas forest actually exhibiting decreasing K_s with tree height, with a slope of -0.25 (Fig. 3c).

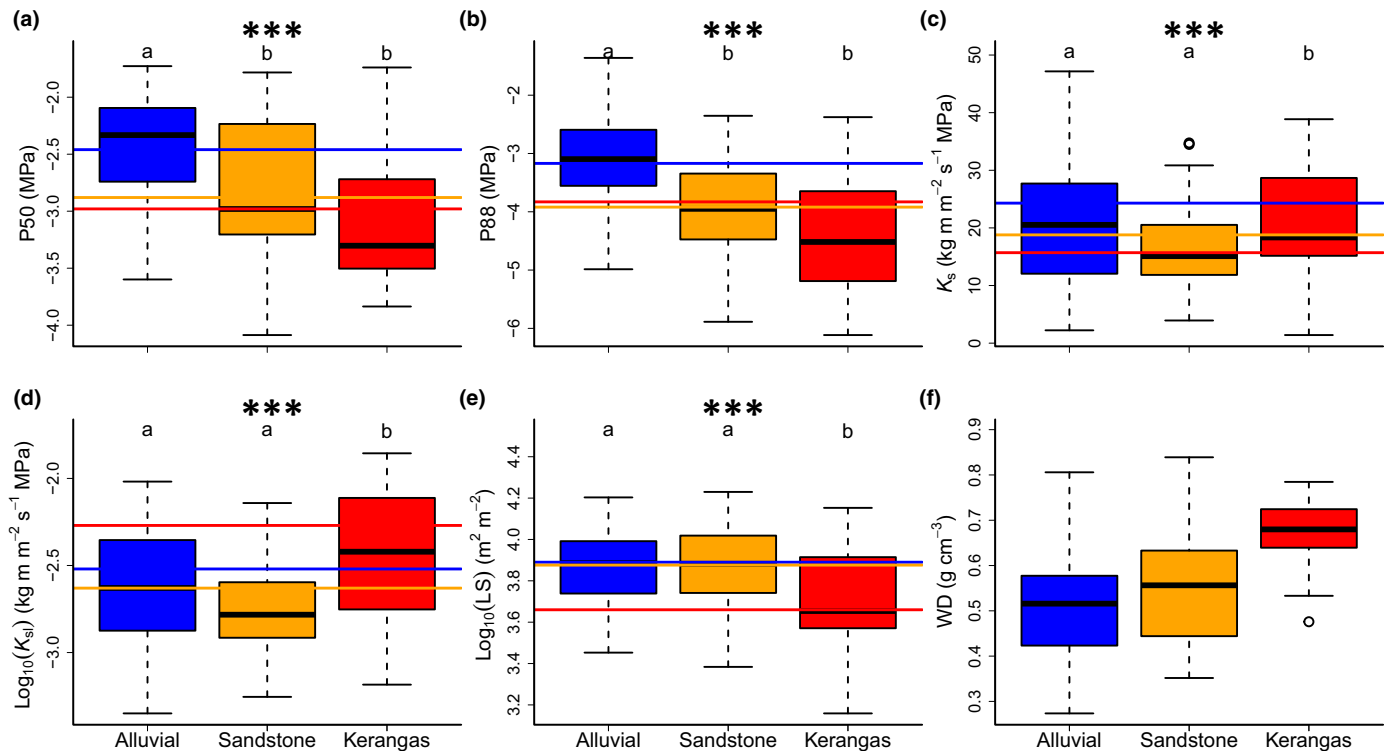


Fig. 2 Hydraulic traits of dipterocarp trees measured in three forest types (13 species per forest, *c.* 150 trees samples across all sampled tree heights; significant differences relate to the mixed model analyses, with species as a random effect when significant (see Table 2 for statistics and model structure)). (a, b) Water potential causing 50% and 88% reductions in hydraulic conductivity (P50 and P88); (c) maximum specific hydraulic conductivity ($K_{s,max}$); (d) maximum leaf specific hydraulic conductivity ($K_{s,leaf}$); (e) leaf : sapwood area ratio (LS); (f) wood density (WD). The box represents quartiles 1 and 3, with the central line indicating the mean. Whiskers are either maximum values or 1.5× the interquartile range above quartile 3, when outliers are present. Traits for which forest type had a significant fixed effect, within the mixed model analysis, are marked with asterisks (***, $P < 0.001$). Forest types with significantly different trait values are marked with different lowercase letters above their boxes. Note that this figure represents our data distribution along only one of the effects we tested (forest type), while our design and the model we tested are multidimensional (see Table 2). The horizontal lines indicate the mixed model's group predictions for a 40-m tall tree for the alluvial, sandstone and kerangas forest types (blue, orange and red lines), when a fixed effect is significant. Different lowercase letters denote significant differences amongst forest type groups in the models. The box represents quartiles 1 and 3, with the central line indicating the median. Whiskers are either maximum values or 1.5× the interquartile range beyond the quartiles, when outliers are present.

Changes in hydraulic trait coordination across forest types

We used SMA to analyse whether the intercept and slope of dipterocarp hydraulic trait relationships were modulated by the forest type in which they occurred. We found that hydraulic trait coordination for many dipterocarp trees varied amongst forest types, either because bivariate trait–trait relationships were only significant in a subset of forest types, or because the relationships had different slopes or intercepts across forests (Fig. 4; Table 3). Among the traits which are expected to be strongly related because they are methodologically linked, $K_{s,leaf}$ –LS had their slope change significantly with forest type ($P < 0.001$; Fig. 4m), while K_s – $K_{s,leaf}$ and P50–P88 maintained a similar slope across forests, but with varying intercepts ($P = 0.002$ and $P = 0.021$, Fig. 4a,j).

For the hydraulic traits that are methodologically independent, the P50– K_s and P88– K_s coordinated with significant positive slopes, but only for the alluvial forest ($P = 0.004$ and $P = 0.014$; Fig. 4b,f); P50– $K_{s,leaf}$ and P88– $K_{s,leaf}$ also had a positive slope in the alluvial forest ($P < 0.001$; Fig. 4c,g). The P50–LS coordination was significant for the alluvial and sandstone forests ($P =$

0.003 and $P = 0.024$; Fig. 4d), with similar slopes and intercepts ($P = 0.15$), indicating that the relationship was consistent across forest types. The P50–WD and P88–WD relationships were significant and negative in the sandstone and kerangas forests, but not in the alluvial forest (Fig. 4e,i), with different intercepts for P50–WD and different slopes for P88–WD ($P = 0.01$ and $P = 0.005$). K_s decreased with LS for the kerangas forest only ($P = 0.16$; Fig. 4k), while $K_{s,leaf}$ decreased with LS in all forest types (Fig. 4m), and different forests had different slopes ($P < 0.001$). K_s , $K_{s,leaf}$ and LS were not related to WD for any forest type ($P > 0.10$; Fig. 4l,n,o).

Discussion

We investigated how hydraulic traits varied in trees growing in climatically identical but edaphically varied forest habitats in Borneo to identify whether variation in these traits is explained by differential species habitat associations and tree size. Our data reveal that variability in the hydraulic traits of dipterocarp trees is being driven by a complex combination of topographic–edaphic conditions, tree height and taxonomic identity. Embolism

Table 2 Linear mixed models for six hydraulic traits, explained by the fixed effects of forest type (alluvial, sandstone and kerangas), tree height (m), tree height and forest type interaction ($S \times \text{Height}$ and $K \times \text{Height}$) and random effects accounting for variation in the intercept among species (1|species) and in the slope of the species-by-tree height interaction (species:height).

Response	Fixed effects					Random effects						
	Intercept	Height	$S \times \text{Height}$	$K \times \text{Height}$	Sandstone	Kerangas	P	(1 species)	(species:height)	P	R_m^2	R_c^2
P50	-2.46 ± 0.13				-0.42 ± 0.15	-0.42 ± 0.19	0.002	0.55	0.01	< 0.001	0.12	0.61
P88	-3.17 ± 0.17				-0.75 ± 0.19	-0.66 ± 0.27	< 0.001	0.41		< 0.001	0.18	0.41
K_s	13.1 ± 3.0	0.28 ± 0.07	-0.18 ± 0.11	-0.53 ± 0.16	1.69 ± 4.13	12.6 ± 4.82	0.002	4.3		0.002	0.14	0.34
$\log_{10}(K_{s,\text{leaf}})$	-2.88 ± 0.07	0.009 ± 0.002			-0.11 ± 0.06	0.25 ± 0.06	< 0.001			0.27	0.27	0
$\log_{10}(\text{LS})$	3.89 ± 0.03				-0.014 ± 0.04	-0.23 ± 0.04	< 0.001		0.002	0.006	0.34	0.52
WD	0.57 ± 0.03						0.12	0.13	0.002	< 0.001	0	0.70

Values for fixed effects are fitted parameter \pm SE of the mean. $S \times \text{Height}$ and $K \times \text{Height}$ are, respectively, the sandstone and kerangas forest effect on the height effect (i.e. their interaction). Values for random effects are the SD of the normal distribution describing the random effect. R_c^2 and R_m^2 are the conditional and marginal model coefficients of determination. Blank cells indicate that the effect is not significant.

K_s , maximum hydraulic specific conductivity ($\text{kg m m}^{-2} \text{s}^{-1} \text{MPa}^{-1}$); $K_{s,\text{leaf}}$, maximum hydraulic leaf-specific conductivity ($\text{kg m m}^{-2} \text{s}^{-1} \text{MPa}^{-1}$); LS, leaf : sapwood area ratio ($\text{m}^2 \text{m}^{-2}$); P50, water potential causing a 50% reduction in hydraulic conductivity (MPa); P88, water potential causing an 88% reduction in hydraulic conductivity (MPa); WD, wood density (g cm^{-3}).

resistance and hydraulic efficiency correspond to the edaphic habitat preferences of different dipterocarp species, with plants in drier conditions having higher embolism resistance and lower hydraulic efficiency. This could be limiting the niche space they can occupy across the gradient from wet clay soils to drier, sandy soils. By contrast, we find that only traits related to water transport efficiency and capacity vary with height, most likely because they are key traits enabling taller trees to adjust to greater height-induced hydraulic limitations. These results suggest that dipterocarp hydraulic traits show independent adaptive responses to both tree height and topographic–edaphic conditions. Furthermore, hydraulic trait–trait relationships were also modulated by forest type, suggesting that selection by topographic–edaphic conditions occurs not only on singular traits, but on multivariate trait relationships which determine plant function. Our data suggest that hydraulic traits play a significant role in shaping the topographic–edaphic and the canopy position dipterocarps species specialize to.

Embolism resistance explains dipterocarp species niche specialization

Alluvial forest dipterocarp species exhibited the greatest vulnerability to embolism, as measured by P50, with values on average *c.* 0.42 MPa higher than those found in the kerangas and in the sandstone forest dipterocarps. Embolism resistance is known to be strongly selected for by climatological aridity, with drier sites driving the evolution of species with lower P50 (Blackman *et al.*, 2014; Larter *et al.*, 2017). As the studied sites share the same climate, the large differences in soil conditions along the gradient must be driving these functional changes. The sandier soils of the kerangas and sandstone forests are likely to create more water-limited conditions, compared with the alluvial forest, despite the same climatological water availability. Unlike most of the Amazon, where seasonality can be intense and interannual variability can lead to periodic drought (Lopes *et al.*, 2016), monthly precipitation in Bornean forests rarely drops below 100 mm, and water deficits are likely to be relatively minor or occur sporadically, for example in association with El Niño events (Guan *et al.*, 2015; Fig. S1). However, these infrequent climatologically dry spells are likely to result in more intense water shortages in the kerangas and sandstone forests, where soils hold less water. Results from one other study looking at plant hydraulic traits across soil gradients in Bornean forests (Tyree *et al.*, 1998) showed a similar trend in embolism resistance (P50) for a sandier forest and a forest on a more clay-rich soil ($P = 0.11$). Their work was based on a much smaller sampling effort (one individual of 14 species per site) and the trees sampled were juveniles (< 5 cm DBH), which could be the reason for its marginally significant results. In the Central Amazon, trees in sandier soils in valleys, close to the water table, were shown in previous studies (Oliveira *et al.*, 2019; Fontes *et al.*, 2020) to have lower embolism resistance than trees growing on clayey soils farther from the water table; by contrast, we found trees growing on more clay-rich soils in Sepilok to have lower embolism resistance. Together, these results suggest that water availability rather than

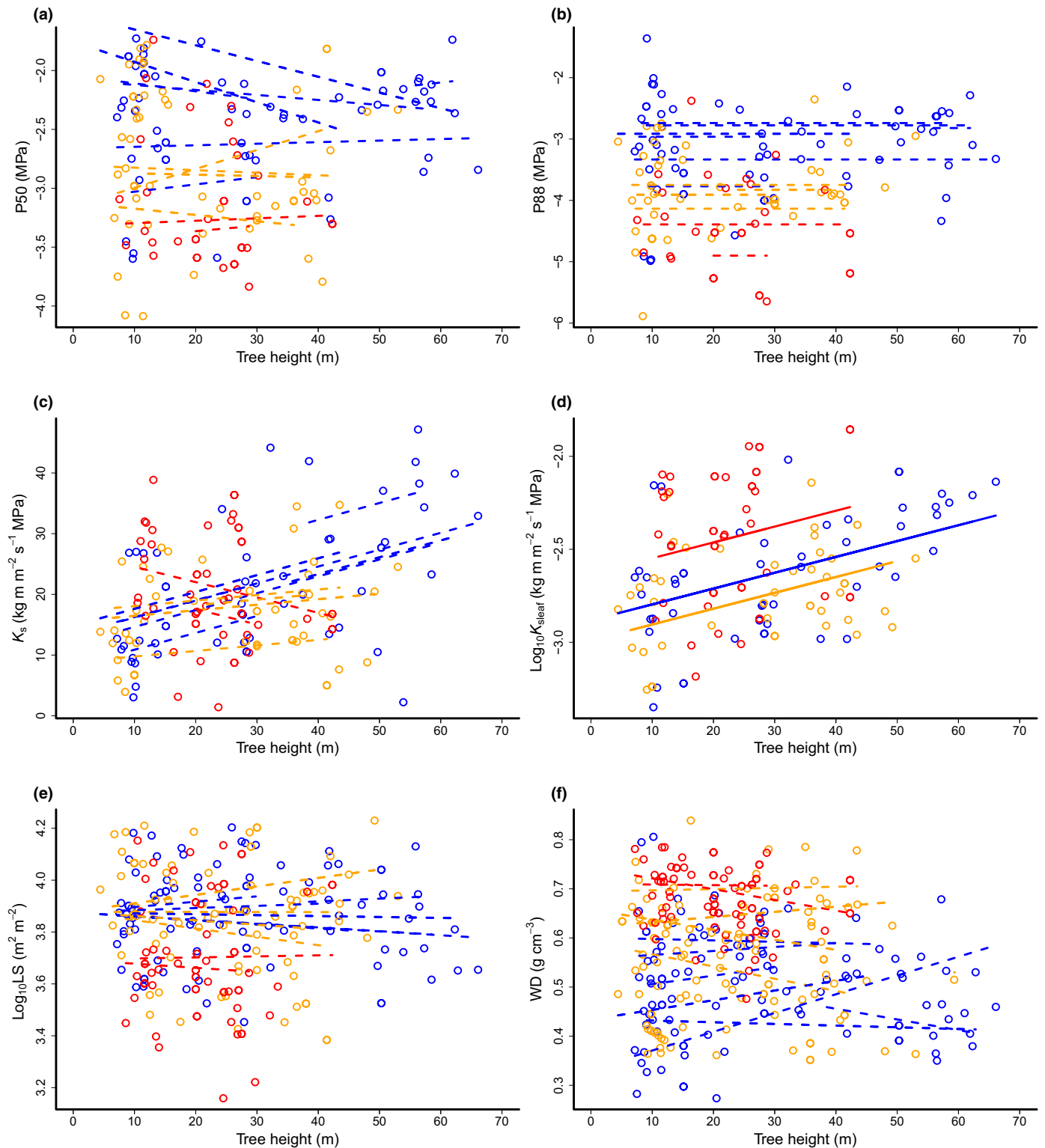


Fig. 3 Tree height effects on dipterocarp hydraulic traits. (a, b) Water potential causing 50% and 88% reductions in hydraulic conductivity (P50 and P88); (c) maximum specific hydraulic conductivity (K_s); (d) maximum leaf specific hydraulic conductivity (K_{sleaf}); (e) leaf : sapwood area ratio (LS); (f) wood density (WD). Data point colour indicates data from different forest types: alluvial (blue), sandstone (orange) or kerangas (red). The significant model effects are represented as lines (see Table 2 for a statistical summary), with dashed coloured lines indicating random plus fixed effects for individual dipterocarp species and solid lines in (d) indicating the fixed effect only, as for this variable there was no significant random effect.

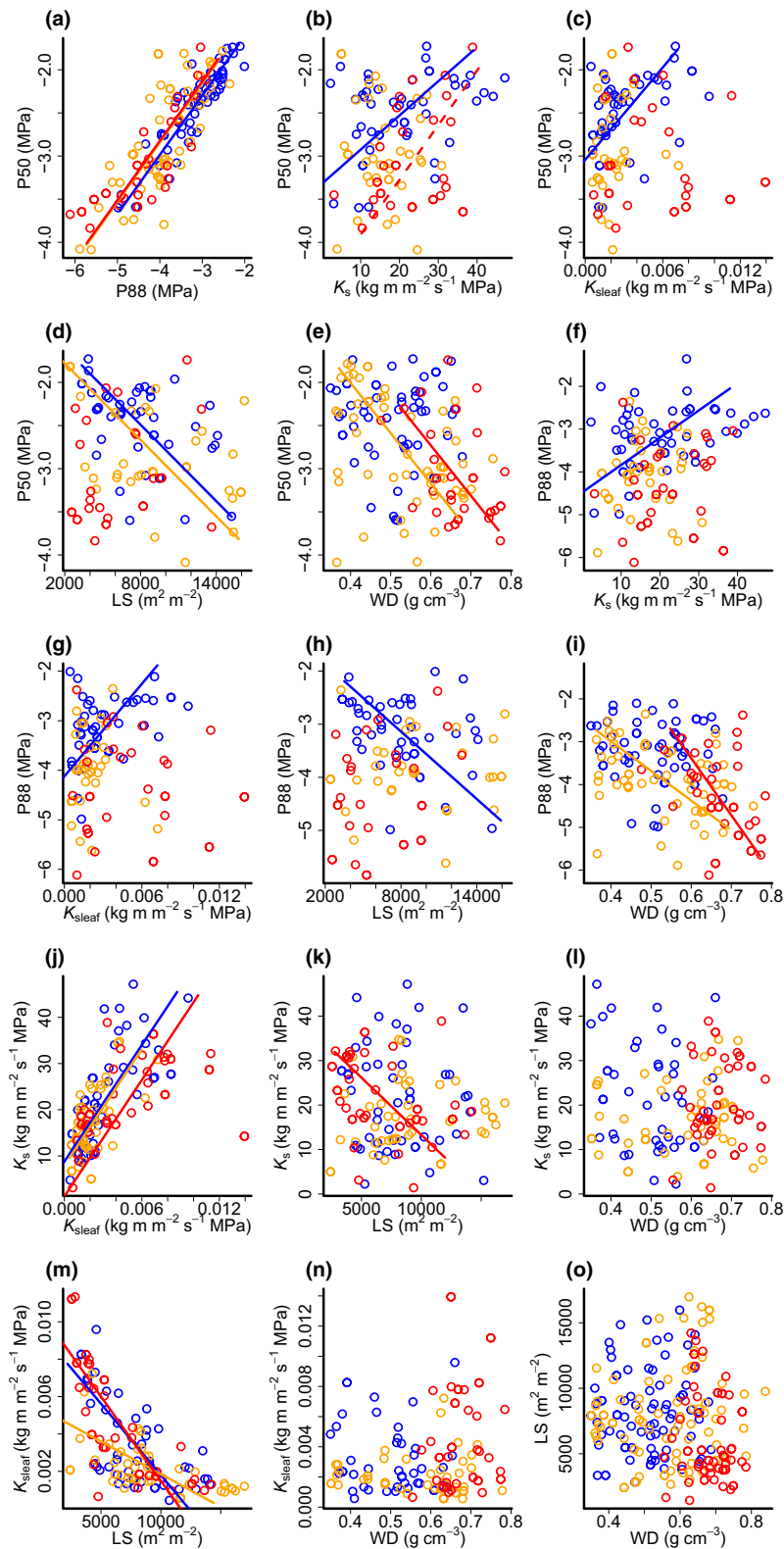


Fig. 4 Standardised major axis regression for hydraulic trait interactions and its modulation by forest type. (a–e) Relationship between P50 and P88, K_s , K_{sleaf} , LS and WD; (f–i) relationship between P88 and K_s , K_{sleaf} , LS and WD; (j–l) relationship between K_s and K_{sleaf} , LS and WD; (m) and (n) relationship between K_{sleaf} and LS and WD; (o) relationship between LS and WD. Forest type is represented by data and line colours (alluvial – blue, sandstone – orange, kerangas – red). Continuous coloured lines represent the significant relationships of the fitted models and dashed lines represent marginally significant relationships ($0.05 < P < 0.06$). Significance values and fitted parameters for each model are presented in Table 3. K_s , maximum hydraulic specific conductivity ($\text{kg m}^{-2} \text{s}^{-1} \text{MPa}^{-1}$); K_{sleaf} , maximum hydraulic leaf-specific conductivity ($\text{kg m}^{-2} \text{s}^{-1} \text{MPa}^{-1}$); LS, leaf : sapwood area ratio ($\text{m}^2 \text{m}^{-2}$); P50 and P88, water potential causing 50% and 88% reduction in hydraulic conductivity (MPa); WD, wood density (g cm^{-3}).

soil texture *per se* is most critical in selecting for embolism resistance. If trees in the kerangas forest were to invest in a higher density of fine roots relative to the trees in other forests (which has been observed, D. F. R. P. Burslem, pers. obs.), they may partially overcome the water transport limitation in the soil, as

suggested by the model of Sperry *et al.* (1998). This would make xylem adaptations an effective way to prevent embolism and maintain water transport.

However, we also found K_s and K_{sleaf} to be *c.* 96% and *c.* 78% higher for trees growing in the kerangas forest, relative to the

Table 3 Results of the standardised major axis regression models, testing whether relationships between dipterocarp hydraulic traits are modulated by forest type (A = alluvial, S = sandstone and K = kerangas).

Hydraulic traits	Coordination-P			Intercept			Slope			Pairwise-P			r^2			
	A	S	K	A	S	K	A	S	K	A-S	A-K	S-K	A	S	K	
	< 0.001	< 0.001	< 0.001	-0.23	0.09	0.07	0.69	0.69	0.69	0.69	0.02	0.06	0.76	0.84	0.55	0.70
P88	< 0.001	< 0.001	< 0.001	-0.23	0.09	0.07	0.69	0.69	0.69	0.02	0.06	0.76	0.84	0.55	0.70	
K_s	0.02	0.36	0.067	-3.32		-4.54	0.04	0.06	0.004	0.001	0.36	0.04	0.11	0.11		
K_{sleaf}	0.002	0.64	0.55	-3.04		178.2			< 0.001	< 0.001	0.70	< 0.001	0.20			
LS	0.003	0.024	0.19	-1.31	-1.48		-0.00014	-0.00014	0.33	< 0.001	0.15	< 0.001	0.19	0.15		
WD	0.86	< 0.001	0.025	-4.47	0.33	0.77	-5.83	-5.83	0.30	0.01	0.1	0.09	0.03	0.19	0.15	
K_s	0.02	0.41	0.56	-4.47			0.064		0.014	0.011	0.97	0.018	0.10			
K_{sleaf}	0.01	0.27	0.95	-3.01			2.32		0.33	< 0.001	0.003	0.003	0.13			
P88	0.015	0.99	0.15	-1.45			-0.0002		0.334	0.25	0.08	0.01	0.13			
WD	0.42	0.012	0.017	-0.21	-4.6		-6.93	-13.3	0.005	0.46	0.013	0.002	0.11	0.15		
K_{sleaf}	< 0.001	< 0.001	< 0.001	96.5	95.1	91.1	12.3	12.3	0.08	0.47	< 0.001	0.04	0.59	0.41	0.43	
LS	0.56	0.54	0.016		39.0			0.003	0.008	0.002	0.08	0.15	0.13			
K_s	0.12	0.63	0.58													
K_{sleaf} ($\times 10^3$)	LS	< 0.001	< 0.001	9.4	5.3	10.5	0.007	0.003	< 0.001	< 0.001	0.29	< 0.001	0.37	0.33	0.59	
K_{sleaf} ($\times 10^3$)	WD	0.33	0.97	0.49												
LS	WD	0.67	0.09	0.11												

Models were fitted with forest type affecting both the intercept and slope of the trait–trait relationships. When trait–trait relationships were significant in at least one forest type (coordination- P < 0.05), we tested for the effect of forest type on the slope of trait coordination. Slope- P is the probability of the trait–trait relationship of the different forest types having the same slope. When forest type did not have a significant effect on the slope of the trait coordination, we refitted the models for the effect of forest type on the intercept of trait relationship. Intercept- P is the probability of the relationship between traits in different forests having the same intercept. Pair-wise- P is the probability of two different forest types having similar slopes (if slope differences are significant) or intercepts (if intercept differences are significant). r^2 is the coefficient of determination of the different models. Bold values highlight significant forest-level interactions, and italics indicate marginally significant interactions ($P < 0.07$). For nonsignificant relationships, entries are left blank. Note that the left hydraulic traits column was fitted as the y-axis in the model. A, alluvial forest; K, kerangas forest; K_s , maximum hydraulic specific conductivity ($\text{kg m}^{-2} \text{s}^{-1} \text{MPa}^{-1}$); K_{sleaf} , maximum hydraulic leaf-specific conductivity ($\text{kg m}^{-2} \text{s}^{-1} \text{MPa}^{-1}$); LS, leaf : sap-wood area ratio ($\text{m}^2 \text{m}^{-2}$); P50, water potential causing a 50% reduction in hydraulic conductivity (MPa); P88, water potential causing an 88% reduction in hydraulic conductivity (MPa); S, sandstone forest; WD, wood density (g cm^{-3}).

alluvial and sandstone forests (Fig. 2). We expected trees in the alluvial and sandstone forests to have higher hydraulic efficiency and capacity than those in the kerangas forest to support their denser canopies and greater heights (Jucker *et al.*, 2018). Trees in the kerangas forest also had lower LS, which further increases leaf water supply capacity and highlights the importance of tree allometry to water transport (Martínez-Vilalta *et al.*, 2009; Petit *et al.*, 2018; Mencuccini *et al.*, 2019). We note these results are not artefacts of different tree sizes in these forests, as we controlled for tree height in our analyses. Unexpectedly, we found no relationship between K_s and P50 in the kerangas forest, which would suggest that there is no discernible safety–efficiency trade-off among trees growing in this environment and allows the kerangas forest trees to have both higher K_s and lower P50 than those in the other forests (Fig. 4). This result, together with the higher embolism resistance of the kerangas forest trees, strongly suggests that the sandier soils in this forest are more hydraulically challenging, requiring both greater embolism resistance to cope with soil water deficits and higher water transport capacity to avoid significant water potential drops and embolism.

Very few dipterocarp species occur in the kerangas forest (Fig. 1), and its tree flora is generally depauperate compared to that of mixed dipterocarp forest across Southeast Asia (Ashton, 2014). These patterns in tree species richness suggest that the traits required for survival in this hydrologically drier site are uncommon within the dipterocarp lineage and are rare within most other families represented in the Southeast Asian tree flora. Dipterocarp species with low embolism resistance and water transport capacity are likely to be constrained to wetter environments, otherwise frequent vessel embolization would either kill them or lead to a very high cost of replacing embolized xylem tissue (Eller *et al.*, 2018). This may also explain why individuals of species generally found only in alluvial or sandstone forests are only found in kerangas forests along the banks of streams (from plot inventory data, not shown).

Changes in hydraulic efficiency and capacity with height

Hydraulic efficiency, as measured by K_s , is a trait linked to how efficiently plants use their xylem volume for water transport (Cruziat *et al.*, 2002; Sperry *et al.*, 2008; Bittencourt *et al.*, 2016). Greater K_s allows a plant to supply the same leaf area using a smaller volume of xylem tissue or over a longer distance with the same amount of tissue investment. We found that dipterocarp trees in the alluvial and sandstone forests adjust to being taller by increasing the hydraulic efficiency (K_s) in their terminal branches, resulting in higher water transport capacity (K_{sleaf}) in the canopies of taller trees (Fig. 3). This indicates that dipterocarp trees compensate for increasing hydraulic resistance with height by adjusting their anatomy, as predicted by scaling studies (West *et al.*, 1999; Sperry *et al.*, 2008; Olson *et al.*, 2009, 2014). Decreases in LS with height were not found (Fig. 3d) in the alluvial and sandstone forests, which suggests that the increases in K_{sleaf} with height were driven by adjustments to K_s , rather than morphological adjustments in LS. This capacity to compensate for increased height through adjusting K_s , without

adjusting LS, may also allow trees to have more flexibility to maintain their carbon balance (photosynthetic gain from leaf area and respiratory cost of sapwood) and biomechanical support, all of which change with LS (Poyatos *et al.*, 2007; Loehle, 2016; Pratt & Jacobsen, 2016; Lehnebach *et al.*, 2018). However, we acknowledge that we were only able to measure sapwood area, rather than fully quantifying the hydraulic pathway by measuring branch length and volume, which is likely to drive the supply–demand dynamics within trees more directly (Anfodillo *et al.*, 2013). This could explain why we found no relationship between LS and tree height for the kerangas forest trees. Trees in the kerangas forest had a decrease in K_s with tree height, but the K_{sleaf} still increased with tree height, suggesting that adaptations to allometry, in addition to adaptations in hydraulic efficiency, might play an important role in adaptation to maintain leaf water supply function with increasing tree size. Shorter trees having higher K_s in these forests may be an adaptation to the limiting water conditions of the sandy soil, meaning rapid uptake is needed before the water infiltrates to lower soil layers. The capacity of dipterocarp trees to adapt K_s and presumably vessel anatomy to achieve greater height is likely to have a lower net carbon cost than adapting allometric ratios (i.e. adding more water transport tissue or decreasing leaf area). It is therefore possible that the maximal limit on this K_s adjustment may be key in determining maximum tree height in dipterocarps.

Increasing embolism resistance with tree height was dependent on species identity rather than a universal family-level strategy, as found in Eastern Amazonian tree species (Bittencourt *et al.*, 2020). Increases in embolism resistance with height are hypothesised to be a necessary adjustment to compensate for the following: gravity-induced decreases in tree water potential with height (Bennett *et al.*, 2015; Couvreur *et al.*, 2018), water potential drops arising from vessel widening not fully compensating for height-related increases in resistance (Poyatos *et al.*, 2007; Liu *et al.*, 2019), and declines in water potential associated with the drier atmospheric conditions found higher up in forest canopies (Kumagai *et al.*, 2001; Bennett *et al.*, 2015). Our results support the idea that adjustments in embolism resistance do not represent a general strategy for trees to deal with water stress from increasing tree height. Our results therefore suggest that different hydraulic traits are being selected for in dipterocarp trees to adjust to vertical vs horizontal variation in environments, with hydraulic efficiency and embolism resistance additively, but independently, modulating dipterocarp hydraulic function.

Hydraulic trait networks are modulated by the environment of dipterocarp trees

Hydraulic traits are not independent, and variation in one trait can result in changes in another hydraulic trait or influence traits relating to other functions, such as carbon assimilation or biomechanics (Pratt & Jacobsen, 2016; Olson *et al.*, 2018). Similarly, multiple distinct selective pressures, such as selection for being tall and for survival on drier soils, may act simultaneously but in different directions on overlapping sets of traits. This could cause significant spatial variation in trait coordination with varying

environmental conditions and forest structural changes. We tested the hypothesis that hydraulic trait relationships are not universal, but rather are modulated by forest type, finding multiple instances where trait coordination changed across habitat types within the dipterocarp species we studied (Fig. 4). We found that key hydraulic trait relationships that are commonly reported in the literature, such as P50–wood density and P50– K_{sleaf} (Markesteijn *et al.*, 2011; Reich, 2014; Christoffersen *et al.*, 2016), were altered in terms of slope, intercept and strength between the three forest types. One of the key hydraulic trait relationships, which is highly relevant to the hydraulic niche that a tree occupies, is the trade-off between hydraulic safety (embolism resistance – P50) and hydraulic efficiency (hydraulic specific conductivity – K_s ; Gleason *et al.*, 2016). Our results show that this trade-off seems to be context dependent and only significant for dipterocarps in the alluvial forests (P50; Fig. 4), possibly because K_s is under stronger selection in an environment that supports trees expressing greater variation in height. This may, in part, explain why global analyses find weak relationships between hydraulic safety (P50) and hydraulic efficiency (K_s) in comparisons across multiple sites that vary in environmental conditions (Gleason *et al.*, 2016).

Conclusions

Dipterocarp hydraulic traits change with both local topographic–edaphic conditions and tree height. Our study shows that embolism resistance varies substantially amongst dipterocarp species found in forests with different topographic–edaphic conditions, under the same climatic conditions. These differences may determine the capacity for species to survive in environments with differential soil water availability and may contribute to the significant spatial turnover and evidence of niche specialization observed along those fine-scale environmental gradients. Hydraulic capacity was influenced by both habitat type and tree height, resulting from adjustments in hydraulic efficiency, reflecting patterns of tree allometry. The tallest tropical trees therefore did not adjust their capacity for resisting embolisms with height, but increased their water transport capacity to compensate for the increased resistance to water transport with size. The strong habitat relationship with embolism resistance and size relationship with water transport efficiency meant that a universal hydraulic safety–efficiency trade-off was not found across these forests, although it was expressed within the wetter alluvial forest. Critically, habitat affiliation of the dipterocarp species also had a considerable impact on hydraulic trait relationships, which varied substantially between habitat types. This evidence demonstrates the importance of plant hydraulic traits for controlling both vertical and spatial niche occupancy within Southeast Asian dipterocarp forests.

Acknowledgements

PRdLB acknowledges the Royal Society for its Newton International Fellowship (NF170370) and LR acknowledges a UK NERC independent fellowship grant NE/N014022/1. DCB

acknowledges UK NERC NE/L002434/1 for its studentship. We are grateful for the logistic and scientific support of the Forest Research Centre, Sabah Forestry Department, and in particular to Noreen Majalap and Rolando Robert. We thank the Sabah Biodiversity Centre and the Sabah Forestry Department for permission to conduct this research in Sepilok Forest Reserve (access permit JKM/MBS.1000-2/2 JLD.9 (17)).

Author contributions

PRdLB, LR, LFB and DFRPB conceived the research ideas and developed the project. PRdLB and DCB collected the data. PRdLB analysed the data and wrote the manuscript. PRdLB, LR, LFB, DFRPB, MAFBS and RN contributed to manuscript preparation.

ORCID

Lindsay F. Banin  <https://orcid.org/0000-0002-1168-3914>
 Paulo Roberto de Lima Bittencourt  <https://orcid.org/0000-0002-1618-9077>
 Lucy Rowland  <https://orcid.org/0000-0002-0774-3216>

Data availability

The data that support the findings of this study are available at <https://doi.org/10.5061/dryad.w6m905qrs>.

References

- Anfodillo T, Petit G, Crivellaro A. 2013. Axial conduit widening in woody species: a still neglected anatomical pattern. *LAWA Journal* 34: 352–364.
- Ashauer M, Glosch H, Hedrich F, Hey N, Sandmaier H, Lang W. 1999. Thermal flow sensor for liquids and gases based on combinations of two principles. *Sensors and Actuators A: Physical* 73: 7–13.
- Ashton, P. 2014. *On the forests of tropical Asia. Let the memory fade*. Richmond, Surrey, UK: Royal Botanic Gardens Kew, 670.
- Avitabile V, Herold M, Heuvelink GBM, Lewis SL, Phillips OL, Asner GP, Armston J, Ashton PS, Banin L, Bayol N *et al.* 2016. An integrated pan-tropical biomass map using multiple reference datasets. *Global Change Biology* 22: 1406–1420.
- Baldeck CA, Harms KE, Yavitt JB, John R, Turner BL, Valencia R, Navarrete H, Davies SJ, Chuyong GB, Kenfack D *et al.* 2013. Soil resources and topography shape local tree community structure in tropical forests. *Proceedings of the Royal Society B: Biological Sciences* 280: 20122532.
- Baltzer JL, Thomas SC, Nilus R, Burslem DFRP. 2005. Edaphic specialization in tropical trees: physiological correlates and responses to reciprocal transplantation. *Ecology* 86: 3063–3077.
- Banin L, Feldpausch TR, Phillips OL, Baker TR, Lloyd J, Affum-Baffoe K, Arets EJMM, Berry NJ, Bradford M, Brienen RJW *et al.* 2012. What controls tropical forest architecture? Testing environmental, structural and floristic drivers: determinants of tropical forest architecture. *Global Ecology and Biogeography* 21: 1179–1190.
- Barros FV, PRL B, Brum M, Restrepo-Coupe N, Pereira L, Teodoro GS, Saleska SR, Borma LS, Christoffersen BO, Penha D *et al.* 2019. Hydraulic traits explain differential responses of Amazonian forests to the 2015 El Niño-induced drought. *New Phytologist* 223: 1253–1266.
- Bartholomew DC, Banin LF, Bittencourt PRL, Suis MAF, Mercado LM, Nilus R, Burslem DFRP, Rowland LR. 2022. Differential nutrient limitation controls leaf physiology, supporting niche partitioning in tropical dipterocarp forests. *Functional Ecology*. doi: 10.1111/1365-2435.14094.

- Barton K. 2016. *MUMIN: multi-model inference*. [WWW document] URL <https://cran.r-project.org/web/packages/MuMIn/index.html> [accessed 6 June 2020].
- Bennett AC, McDowell NG, Allen CD, Anderson-Teixeira KJ. 2015. Larger trees suffer most during drought in forests worldwide. *Nature Plants* 1: 15139.
- Bittencourt P, Pereira L, Oliveira R. 2018. Pneumatic method to measure plant xylem embolism. *Bio-Protocol* 8: e2059.
- Bittencourt PR, Pereira L, Oliveira RS. 2016. On xylem hydraulic efficiencies, wood space-use and the safety–efficiency tradeoff. *New Phytologist* 211: 1152–1155.
- Bittencourt PRL, Oliveira RS, da Costa ACL, Giles AL, Coughlin I, Costa PB, Bartholomew DC, Ferreira LV, Vasconcelos SS, Barros FV *et al.* 2020. Amazonian trees have limited capacity to acclimate plant hydraulic properties in response to long-term drought. *Global Change Biology* 26: 3569–3584.
- Blackman CJ, Brodribb TJ, Jordan GJ. 2011. Leaf hydraulic vulnerability influences species' bioclimatic limits in a diverse group of woody angiosperms. *Oecologia* 168: 1–10.
- Blackman CJ, Gleason SM, Chang Y, Cook AM, Laws C, Westoby M. 2014. Leaf hydraulic vulnerability to drought is linked to site water availability across a broad range of species and climates. *Annals of Botany* 114: 435–440.
- Brearley FQ, Banin LF, Saner P. 2016. The ecology of the Asian dipterocarps. *Plant Ecology & Diversity* 9: 429–436.
- Brodribb TJ, McAdam SA, Carins Murphy MR. 2017. Xylem and stomata, coordinated through time and space: functional linkages between xylem and stomata. *Plant, Cell & Environment* 40: 872–880.
- Choat B, Sack L, Holbrook NM. 2007. Diversity of hydraulic traits in nine *Cordia* species growing in tropical forests with contrasting precipitation. *New Phytologist* 175: 686–698.
- Christoffersen BO, Gloor M, Fauset S, Fyllas NM, Galbraith DR, Baker TR, Rowland L, Fisher RA, Binks OJ, Sevanto SA *et al.* 2016. Linking hydraulic traits to tropical forest function in a size-structured and trait-driven model (TFS v.1-Hydro). *Geoscientific Model Development Discussions* 9: 4227–4255.
- Copernicus Climate Change Service. 2019. *ERA5-Land monthly averaged data from 2001 to present*. [WWW document] URL <https://cds.climate.copernicus.eu/cdsapp#!/dataset/reanalysis-era5-land-monthly-means?tab=overview> [accessed 6 June 2020].
- Cosme LHM, Schiatti J, Costa FRC, Oliveira RS. 2017. The importance of hydraulic architecture to the distribution patterns of trees in a central Amazonian forest. *New Phytologist* 215: 113–125.
- Couvreur V, Ledder G, Manzoni S, Way DA, Muller EB, Russo SE. 2018. Water transport through tall trees: a vertically explicit, analytical model of xylem hydraulic conductance in stems: vertically explicit, analytical hydraulic model. *Plant, Cell & Environment* 41: 1821–1839.
- Cruziat P, Cochard H, Améglio T. 2002. Hydraulic architecture of trees: main concepts and results. *Annals of forest science* 59: 723–752.
- Dai A. 2013. Increasing drought under global warming in observations and models. *Nature Climate Change* 3: 52–58.
- Dent DH, Bagchi R, Robinson D, Majalap-Lee N, Burslem DFRP. 2006. Nutrient fluxes via litterfall and leaf litter decomposition vary across a gradient of soil nutrient supply in a lowland tropical rain forest. *Plant and Soil* 288: 197–215.
- Dent DH, Burslem DFRP. 2009. Performance trade-offs driven by morphological plasticity contribute to habitat specialization of Bornean tree species: habitat specialization of tropical tree species. *Biotropica* 41: 424–434.
- Dent DH, Burslem DFRP. 2016. Leaf traits of dipterocarp species with contrasting distributions across a gradient of nutrient and light availability. *Plant Ecology & Diversity* 9: 521–533.
- Eller CB, Rowland L, Mencuccini M, Rosas T, Williams K, Harper A, Medlyn BE, Wagner Y, Klein T, Teodoro GS *et al.* 2020. Stomatal optimization based on xylem hydraulics (SOX) improves land surface model simulation of vegetation responses to climate. *New Phytologist* 226: 1622–1637.
- Eller CB, Rowland L, Oliveira RS, Bittencourt PRL, Barros FV, da Costa ACL, Meir P, Friend AD, Mencuccini M, Sitch S *et al.* 2018. Modelling tropical forest responses to drought and El Niño with a stomatal optimization model based on xylem hydraulics. *Philosophical Transactions of the Royal Society of London. Series B: Biological Sciences* 373: 20170315.
- Esquivel-Muelbert A, Galbraith D, Dexter KG, Baker TR, Lewis SL, Meir P, Rowland L, da Costa ACL, Nepstad D, Phillips OL. 2017. Biogeographic distributions of neotropical trees reflect their directly measured drought tolerances. *Scientific Reports* 7: 8334.
- Esteban EJJ, Castilho CV, Melgaço KL, Costa FRC. 2021. The other side of droughts: wet extremes and topography as buffers of negative drought effects in an Amazonian forest. *New Phytologist* 229: 1995–2006.
- Fajardo A, McIntire EJB, Olson ME. 2019. When short stature is an asset in trees. *Trends in Ecology & Evolution* 34: 193–199.
- Feldpausch TR, Banin L, Phillips OL, Baker TR, Lewis SL, Quesada CA, Affum-Baffoe K, Arets EJM, Berry NJ, Bird M *et al.* 2011. Height-diameter allometry of tropical forest trees. *Biogeosciences* 8: 1081–1106.
- Ferry B, Morneau F, Bontemps J-D, Blanc L, Freycon V. 2010. Higher treefall rates on slopes and waterlogged soils result in lower stand biomass and productivity in a tropical rain forest: treefall and biomass in a tropical rain forest. *Journal of Ecology* 98: 106–116.
- Fisher RA, Williams M, da Costa AL, Malhi Y, da Costa RF, Almeida S, Meir P. 2007. The response of an Eastern Amazonian rain forest to drought stress: results and modelling analyses from a throughfall exclusion experiment. *Global Change Biology* 13: 2361–2378.
- Fontes CG, Fine PVA, Wittmann F, Bittencourt PRL, Piedade MTF, Higuchi N, Chambers JQ, Dawson TE. 2020. Convergent evolution of tree hydraulic traits in Amazonian habitats: implications for community assemblage and vulnerability to drought. *New Phytologist* 228: 106–120.
- Fox JED. 1975. *The natural vegetation of the Sabah and natural regeneration of the Dipterocarp Forests*. PhD thesis, Cardiff, Wales, UK: University of Wales.
- Ghazoul J. 2016. *Dipterocarp biology, ecology, and conservation*. Oxford, UK: Oxford University Press.
- Gleason SM, Westoby M, Jansen S, Choat B, Hacke UG, Pratt RB, Bhaskar R, Brodribb TJ, Bucci SJ, Cao K-F *et al.* 2016. Weak tradeoff between xylem safety and xylem-specific hydraulic efficiency across the world's woody plant species. *New Phytologist* 209: 123–136.
- Guan K, Pan M, Li H, Wolf A, Wu J, Medvigy D, Caylor KK, Sheffield J, Wood EF, Malhi Y *et al.* 2015. Photosynthetic seasonality of global tropical forests constrained by hydroclimate. *Nature Geoscience* 8: 284–289.
- Guan X, Pereira L, McAdam SAM, Cao K, Jansen S. 2021. No gas source, no problem: proximity to pre-existing embolism and segmentation affect embolism spreading in angiosperm xylem by gas diffusion. *Plant, Cell & Environment* 44: 1329–1345.
- Guitet S, Pélissier R, Brunaux O, Jaouen G, Sabatier D. 2015. Geomorphological landscape features explain floristic patterns in French Guiana rainforest. *Biodiversity and Conservation* 24: 1215–1237.
- Hacke UG, Sperry JS, Ewers BE, Ellsworth DS, Schäfer KVR, Oren R. 2000. Influence of soil porosity on water use in *Pinus taeda*. *Oecologia* 124: 495–505.
- Herkelrath WN, Miller EE, Gardner WR. 1977a. Water uptake by plants: II. The root contact model. *Soil Science Society of America Journal* 41: 1039–1043.
- Herkelrath WN, Miller EE, Gardner WR. 1977b. Water uptake by plants: I. Divided root experiments. *Soil Science Society of America Journal* 41: 1033–1038.
- Hultine KR, Koepke DF, Pockman WT, Fravolini A, Sperry JS, Williams DG. 2006. Influence of soil texture on hydraulic properties and water relations of a dominant warm-desert phreatophyte. *Tree Physiology* 26: 313–323.
- Itoh A, Nanami S, Harata T, Ohkubo T, Tan S, Chong L, Davies SJ, Yamakura T. 2012. The effect of habitat association and edaphic conditions on tree mortality during el niño-induced drought in a Bornean dipterocarp forest. *Biotropica* 44: 606–617.
- Itoh A, Yamakura T, Ohkubo T, Kanzaki M, Palmiotto P, Tan S, Lee HS. 2003. Spatially aggregated fruiting in an emergent Bornean tree. *Journal of Tropical Ecology* 19: 531–538.
- Jacobsen AL, Pratt RB, Tobin MF, Hacke UG, Ewers FW. 2012. A global analysis of xylem vessel length in woody plants. *American Journal of Botany* 99: 1583–1591.
- Jucker T, Bongalov B, Burslem DFRP, Nilus R, Dalponte M, Lewis SL, Phillips OL, Qie L, Coomes DA. 2018. Topography shapes the structure, composition and function of tropical forest landscapes. *Ecology Letters* 21: 989–1000.
- Katabuchi M. 2015. LEAFAREA: an R package for rapid digital image analysis of leaf area. *Ecological Research* 30: 1073–1077.
- Katabuchi M, Kurokawa H, Davies SJ, Tan S, Nakashizuka T. 2012. Soil resource availability shapes community trait structure in a species-rich dipterocarp forest. *Journal of Ecology* 100: 643–651.

- Kumagai T, Kuraji K, Noguchi H, Tanaka Y, Tanaka K, Suzuki M. 2001. Vertical profiles of environmental factors within tropical rainforest, Lambir Hills National Park, Sarawak, Malaysia. *Journal of Forest Research* 6: 257–264.
- Larjavaara M, Muller-Landau HC. 2013. Measuring tree height: a quantitative comparison of two common field methods in a moist tropical forest. *Methods in Ecology and Evolution* 4: 793–801.
- Larter M, Pfautsch S, Domec J-C, Trueba S, Nagalingum N, Delzon S. 2017. Aridity drove the evolution of extreme embolism resistance and the radiation of conifer genus *Callitris*. *New Phytologist* 215: 97–112.
- Laughlin DC, Delzon S, Clearwater MJ, Bellingham PJ, McGlone MS, Richardson SJ. 2020. Climatic limits of temperate rainforest tree species are explained by xylem embolism resistance among angiosperms but not among conifers. *New Phytologist* 226: 727–740.
- Lee HS, Davies SJ, LaFrankie J, Tan S, Yamakura T, Itoh A, Ohkubo T, Ashton PS. 2002. Floristic and structural diversity of mixed dipterocarp forest in Lambir Hills National Park, Sarawak, Malaysia. *Journal of Tropical Forest Science* 14: 379–4004.
- Lehnebach R, Beyer R, Letort V, Heuret P. 2018. The pipe model theory half a century on: a review. *Annals of Botany* 121: 773–795.
- Li Y, Xu H, Cohen S. 2005. Long-term hydraulic acclimation to soil texture and radiation load in cotton. *Plant, Cell & Environment* 28: 492–499.
- Liu H, Gleason SM, Hao G, Hua L, He P, Goldstein G, Ye Q. 2019. Hydraulic traits are coordinated with maximum plant height at the global scale. *Science Advances* 5: eaav1332.
- Loehle C. 2016. Biomechanical constraints on tree architecture. *Trees* 30: 2061–2070.
- Lopes AV, Chiang JCH, Thompson SA, Dracup JA. 2016. Trend and uncertainty in spatial-temporal patterns of hydrological droughts in the Amazon basin: hydrological droughts in the Amazon. *Geophysical Research Letters* 43: 3307–3316.
- Markestijn L, Poorter L, Paz H, Sack L, Bongers F. 2011. Ecological differentiation in xylem cavitation resistance is associated with stem and leaf structural traits: vulnerability to cavitation of tropical dry forest tree species. *Plant, Cell & Environment* 34: 137–148.
- Martínez-Vilalta J, Cochard H, Mencuccini M, Sterck F, Herrero A, Korhonen JFJ, Llorens P, Nikinmaa E, Nolè A, Poyatos R *et al.* 2009. Hydraulic adjustment of Scots pine across Europe. *New Phytologist* 184: 353–364.
- McDowell NG, Allen CD. 2015. Darcy's law predicts widespread forest mortality under climate warming. *Nature Climate Change* 5: 669–672.
- Melcher PJ, Michele Holbrook N, Burns MJ, Zwieniecki MA, Cobb AR, Brodribb TJ, Choat B, Sack L. 2012. Measurements of stem xylem hydraulic conductivity in the laboratory and field. *Methods in Ecology and Evolution* 3: 685–694.
- Mencuccini M, Rosas T, Rowland L, Choat B, Cornelissen H, Jansen S, Kramer K, Lapenis A, Manzoni S, Niinemets Ü *et al.* 2019. Leaf economics and plant hydraulics drive leaf: wood area ratios. *New Phytologist* 224: 1544–1556.
- Miller TE, Small H. 1982. Thermal pulse time-of-flight liquid flow meter. *Analytical Chemistry* 54: 907–910.
- Nepstad DC, Tohver IM, Ray D, Moutinho P, Cardinot G. 2007. Mortality of large trees and lianas following experimental drought in an Amazon forest. *Ecology* 88: 2259–2269.
- Nilus R. 2004. *Effect of edaphic variation on forest structure, dynamics, diversity and regeneration in a lowland tropical rain forest in Borneo*. PhD thesis, University of Aberdeen, Aberdeen, UK.
- Oliveira RS, Costa FRC, van Baalen E, de Jonge A, Bittencourt PR, Almanza Y, Barros FV, Cordoba EC, Fagundes MV, Garcia S *et al.* 2019. Embolism resistance drives the distribution of Amazonian rainforest tree species along hydro-topographic gradients. *New Phytologist* 221: 1457–1465.
- Oliveira RS, Eller CB, Barros FV, Hirota M, Brum M, Bittencourt P. 2021. Linking plant hydraulics and the fast–slow continuum to understand resilience to drought in tropical ecosystems. *New Phytologist* 230: 904–923.
- Olson ME, Aguirre-Hernández R, Rosell JA. 2009. Universal foliage-stem scaling across environments and species in dicot trees: plasticity, biomechanics and Corner's rules. *Ecology Letters* 12: 210–219.
- Olson ME, Anfodillo T, Gleason SM, McCulloh KA. 2021. Tip-to-base xylem conduit widening as an adaptation: causes, consequences, and empirical priorities. *New Phytologist* 229: 1877–1893.
- Olson ME, Anfodillo T, Rosell JA, Petit G, Crivellaro A, Isnard S, León-Gómez C, Alvarado-Cárdenas LO, Castorena M. 2014. Universal hydraulics of the flowering plants: vessel diameter scales with stem length across angiosperm lineages, habits and climates. *Ecology Letters* 27: 988–997.
- Olson ME, Rosell JA, Zamora Muñoz S, Castorena M. 2018. Carbon limitation, stem growth rate and the biomechanical cause of Corner's rules. *Annals of Botany* 122: 583–592.
- Paligi SS, Link RM, Isasa E, Bittencourt P, Cabral JS, Jansen S, Oliveira RS, Pereira L, Schuldt B. 2021. Accuracy of the pneumatic method for estimating xylem vulnerability to embolism in temperate diffuse-porous tree species. *BioRxiv*. doi: 10.1101/2021.02.15.431295.
- Pammer NW, Vander Willigen C. 1998. A mathematical and statistical analysis of the curves illustrating vulnerability of xylem to cavitation. *Tree physiology* 18: 589–593.
- Paoli GD, Curran LM, Zak DR. 2006. Soil nutrients and beta diversity in the Bornean Dipterocarpaceae: evidence for niche partitioning by tropical rain forest trees. *Journal of Ecology* 94: 157–170.
- Pereira L, Bittencourt PRL, Oliveira RS, Junior MBM, Barros FV, Ribeiro RV, Mazzafera P. 2016. Plant pneumatics: stem air flow is related to embolism - new perspectives on methods in plant hydraulics. *New Phytologist* 211: 357–370.
- Pereira L, Bittencourt PRL, Pacheco VS, Miranda MT, Zhang Y, Oliveira RS, Groenendijk P, Machado EC, Tyree MT, Jansen S *et al.* 2019. The Pneumatron: an automated pneumatic apparatus for estimating xylem vulnerability to embolism at high temporal resolution. *Plant, Cell & Environment* 49: 131–142.
- Pérez-Harguindeguy N, Díaz S, Garnier E, Lavorel S, Poorter H, Jaureguiberry P, Bret-Harte MS, Cornwell WK, Craine JM, Gurvich DE *et al.* 2013. New handbook for standardised measurement of plant functional traits worldwide. *Australian Journal of Botany* 61: 167.
- Petit G, von Arx G, Kiorapostolou N, Lechthaler S, Prendin AL, Anfodillo T, Caldeira MC, Cochard H, Copini P, Crivellaro A *et al.* 2018. Tree differences in primary and secondary growth drive convergent scaling in leaf area to sapwood area across Europe. *New Phytologist* 218: 1383–1392.
- Phillips OL, Van Der Heijden G, Lewis SL, López-González G, Aragão LE, Lloyd J, Malhi Y, Monteagudo A, Almeida S, Dávila EA *et al.* 2010. Drought–mortality relationships for tropical forests. *New Phytologist* 187: 631–646.
- Pinheiro J, Bates D, DebRoy S, Sarkar D, R Core Team. 2014. *nlme: linear and nonlinear mixed effects models*. R package v.3.1-118. [WWW document] URL <http://CRAN.R-project.org/package=nlme> [accessed 6 June 2020].
- Poeplau C, Kätterer T. 2017. Is soil texture a major controlling factor of root: shoot ratio in cereals?: effect of texture on root:shoot ratio of barley. *European Journal of Soil Science* 68: 964–970.
- Pollacco JAP, Fernández-Gálvez J, Carrick S. 2020. Improved prediction of water retention curves for fine texture soils using an intergranular mixing particle size distribution model. *Journal of Hydrology* 584: 124597.
- Poyatos R, Martínez-Vilalta J, Čermák J, Ceulemans R, Granier A, Irvine J, Köstner B, Lagergren F, Meiresonne L, Nadezhdina N *et al.* 2007. Plasticity in hydraulic architecture of Scots pine across Eurasia. *Oecologia* 153: 245–259.
- Pratt RB, Jacobsen AL. 2016. Conflicting demands on angiosperm xylem: tradeoffs among storage, transport, and biomechanics: tradeoffs in xylem function. *Plant, Cell & Environment* 40: 897–913.
- R Core Team. 2019. *R: a language and environment for statistical computing*. Vienna, Austria: R Foundation for Statistical Computing. [WWW document] URL <https://www.R-project.org/> [accessed 6 June 2020].
- Reich PB. 2014. The world-wide 'fast-slow' plant economics spectrum: a traits manifesto. *Journal of Ecology* 102: 275–301.
- Rowland L, da Costa ACL, Galbraith DR, Oliveira RS, Binks OJ, Oliveira AAR, Pullen AM, Doughty CE, Metcalfe DB, Vasconcelos SS *et al.* 2015. Death from drought in tropical forests is triggered by hydraulics not carbon starvation. *Nature* 528: 119–122.
- Russo SE, Cannon WL, Elowsky C, Tan S, Davies SJ. 2010. Variation in leaf stomatal traits of 28 tree species in relation to gas exchange along an edaphic gradient in a Bornean rain forest. *American Journal of Botany* 97: 1109–1120.
- Ryan MG. 2015. Tree mortality: large trees losing out to drought. *Nature Plants* 1: 15150.

- Sanchez-Martinez P, Martínez-Vilalta J, Dexter KG, Segovia RA, Mencuccini M. 2020. Adaptation and coordinated evolution of plant hydraulic traits. *Ecology Letters* 23: 1599–1610.
- Santiago LS, Goldstein G, Meinzer FC, Fisher JB, Machado K, Woodruff D, Jones T. 2004. Leaf photosynthetic traits scale with hydraulic conductivity and wood density in Panamanian forest canopy trees. *Oecologia* 140: 543–550.
- Savage VM, Bentley LP, Enquist BJ, Sperry JS, Smith DD, Reich PB, von Allmen EI. 2010. Hydraulic trade-offs and space filling enable better predictions of vascular structure and function in plants. *Proceedings of the National Academy of Sciences, USA* 107: 22722–22727.
- Schiatti J, Emilio T, Rennó CD, Drucker DP, Costa FRC, Nogueira A, Baccaro FB, Figueiredo F, Castilho CV, Kinupp V *et al.* 2014. Vertical distance from drainage drives floristic composition changes in an Amazonian rainforest. *Plant Ecology & Diversity* 7: 241–253.
- Schneider CA, Rasband WS, Eliceiri KW. 2012. NIH image to IMAGEJ: 25 years of image analysis. *Nature Methods* 9: 671–675.
- Scholander PF, Hammel HT, Hemmingsen EA, Bradstreet ED. 1964. Hydrostatic pressure and osmotic potential in leaves of mangroves and some other plants. *Proceedings of the National Academy of Sciences, USA* 52: 119.
- Sergent AS, Varela SA, Barigah TS, Badel E, Cochard H, Dalla-Salda G, Delzon S, Fernández ME, Guillemot J, Gyenge J *et al.* 2020. A comparison of five methods to assess embolism resistance in trees. *Forest Ecology and Management* 468: 118175.
- Shenkin A, Chandler CJ, Boyd DS, Jackson T, Disney M, Majalap N, Nilus R, Foody G, bin Jami J, Reynolds G *et al.* 2019. The world's tallest tropical tree in three dimensions. *Frontiers in Forests and Global Change* 2. doi: 10.3389/ffgc.2019.00032
- Slik JWF, Arroyo-Rodríguez V, Aiba S-I, Alvarez-Loayza P, Alves LF, Ashton P, Balvanera P, Bastian ML, Bellingham PJ, van den Berg E *et al.* 2015. An estimate of the number of tropical tree species. *Proceedings of the National Academy of Sciences, USA* 112: 7472–7477.
- Slik JWF, Poulsen AD, Ashton PS, Cannon CH, Eichhorn KAO, Kartawinata K, Lanniari I, Nagamasu H, Nakagawa M, van Nieuwstadt MGL *et al.* 2003. A floristic analysis of the lowland dipterocarp forests of Borneo. *Journal of Biogeography* 30: 1517–1531.
- Sperry JS, Adler FR, Campbell GS, Comstock JP. 1998. Limitation of plant water use by rhizosphere and xylem conductance: results from a model. *Plant, Cell & Environment* 21: 347–359.
- Sperry JS, Donnelly JR, Tyree MT. 1988. A method for measuring hydraulic conductivity and embolism in xylem. *Plant, Cell & Environment* 11: 35–40.
- Sperry JS, Love DM. 2015. What plant hydraulics can tell us about responses to climate-change droughts. *New Phytologist* 207: 14–27.
- Sperry JS, Meinzer FC, McCulloh KA. 2008. Safety and efficiency conflicts in hydraulic architecture: scaling from tissues to trees. *Plant, Cell & Environment* 31: 632–645.
- Sukri RS, Wahab RA, Salim KA, Burslem DFRP. 2012. Habitat associations and community structure of dipterocarps in response to environment and soil conditions in Brunei Darussalam, Northwest Borneo. *Biotropica* 44: 595–605.
- Thomas R, Lello J, Medeiros R, Pollard A, Robinson P, Seward A, Smith J, Vafidis J, Vaughan I. 2017. *Data analysis with R statistical software: a guidebook for scientists*. Newport, UK: Eco-Explore.
- Trueba S, Pouteau R, Lens F, Feild TS, Isnard S, Olson ME, Delzon S. 2017. Vulnerability to xylem embolism as a major correlate of the environmental distribution of rain forest species on a tropical island: embolism vulnerability and rain forest species distribution. *Plant, Cell & Environment* 40: 277–289.
- Tyree MT, Patino S, Becker P. 1998. Vulnerability to drought-induced embolism of Bornean heath and dipterocarp forest trees. *Tree Physiology* 18: 583–588.
- Warton DI, Duursma RA, Falster DS, Taskinen S. 2012. SMATR 3- an R package for estimation and inference about allometric lines: the SMATR 3 - an R package. *Methods in Ecology and Evolution* 3: 257–259.
- West GB, Brown JH, Enquist BJ. 1999. A general model for the structure and allometry of plant vascular systems. *Nature* 400: 664–667.
- Yang D, Pereira L, Peng G, Ribeiro RV, Kaack L, Jansen S, Tyree MT. 2021. A Unit Pipe Pneumatic model to simulate gas kinetics during measurements of embolism in excised angiosperm xylem. *BioRxiv*. doi: 10.1101/2021.02.09.430450.
- Zhang J-L, Cao K-F. 2009. Stem hydraulics mediates leaf water status, carbon gain, nutrient use efficiencies and plant growth rates across dipterocarp species. *Functional Ecology* 23: 658–667.
- Zhang Y, Lamarque LJ, Torres-Ruiz JM, Schuldt B, Karimi Z, Li S, Qin D-W, Bittencourt P, Burlett R, Cao K-F *et al.* 2018. Testing the plant pneumatic method to estimate xylem embolism resistance in stems of temperate trees. *Tree Physiology* 38: 1016–1025.
- Zuur AF, Ieno EN, Walker N, Saveliev AA, Smith GM. 2009. *Mixed effects models and extensions in ecology with R*. New York, NY, USA: Springer.

Supporting Information

Additional Supporting Information may be found online in the Supporting Information section at the end of the article.

Fig. S1 Time series of precipitation (blue, mm), evapotranspiration (orange, mm) and climatological water deficit (red, mm; calculated as in (Barros *et al.*, 2019)) for the Sepilok region from 2003 to 2020.

Fig. S2 Increase in embolism (PGD, percentage air discharge) with increasing branch xylem water potential (Ψ) of dipterocarp individuals in each forest type: (a) alluvial forest, (b) sandstone forest and (c) kerangas forest.

Fig. S3 Relationship between tree height and diameter for dipterocarp trees of the studied species in the alluvial forest (blue), sandstone forest (orange) and kerangas forest (red).

Methods S1 Description of the water flow meter used for maximum hydraulic conductance measurements.

Table S1 Tree density (individuals ha^{-1}), species dominance (% basal area) and dominance rank (by basal area) within all species for each of the studied species in each forest type.

Please note: Wiley Blackwell are not responsible for the content or functionality of any Supporting Information supplied by the authors. Any queries (other than missing material) should be directed to the *New Phytologist* Central Office.